Thermodynamics of Denaturation of Hisactophilin, a β-Trefoil Protein[†]

Chengsong Liu, Dwayne Chu, Rhonda D. Wideman, R. Scott Houliston, Hannah J. Wong, and Elizabeth M. Meiering*

Department of Chemistry, University of Waterloo, Waterloo, Ontario N2L 3G1, Canada

Received November 13, 2000; Revised Manuscript Received February 2, 2001

ABSTRACT: Hisactophilin is a histidine-rich pH-dependent actin-binding protein from *Dictyostelium discoideum*. The structure of hisactophilin is typical of the β-trefoil fold, a common structure adopted by diverse proteins with unrelated primary sequences and functions. The thermodynamics of denaturation of hisactophilin have been measured using fluorescence- and CD-monitored equilibrium urea denaturation curves, pH-denaturation, and thermal denaturation curves, as well as differential scanning calorimetry. Urea denaturation is reversible from pH 5.7 to pH 9.7; however, thermal denaturation is highly reversible only below pH $\sim$ 6.2. Reversible denaturation by urea and heat is well fit using a two-state transition between the native and the denatured states. Urea denaturation curves are best fit using a quadratic dependence of the Gibbs free energy of unfolding upon urea concentration. Hisactophilin has moderate, roughly constant stability from pH 7.7 to pH 9.7; however, below pH 7.7, stability decreases markedly, most likely due to protonation of histidine residues. Enthalpic effects of histidine ionization upon unfolding also appear to be involved in the occurrence of cold unfolding of hisactophilin under relatively mild solution conditions. The stability data for hisactophilin are compared with data on hisactophilin function, and with data for two other β-trefoil proteins, human interleukin-1β, and basic fibroblast growth factor.

Hisactophilin is a histidine-rich, actin-binding protein from the slime mold, *Dictyostelium discoideum* (*1*). This protein is involved in the pH-dependent anchoring of actin to the plasma membrane. In vivo and in vitro experiments have shown that below pH 7 hisactophilin binds to both actin and the cell membrane, while at increased pH, binding is markedly decreased (*1*−*6*). Two-dimensional ^{1}H and ^{15}N NMR titration experiments have revealed that the overall structure of hisactophilin is maintained from pH 5.7 to pH 11.1 and that ionization of histidine residues is implicated in pH-dependent actin and membrane binding (*7*). The histidine residues are located primarily in surface loops, and the overall structure of the protein is typical of the β-trefoil fold family (Figure 1) (*8*, *9*).

We have initiated in depth investigations of the stability and folding of hisactophilin with the aims of elucidating the relationships between stability, folding, and function for hisactophilin, and discerning general features of the stability and folding of β-trefoil proteins. To date, measurements of stability and folding have been reported for two other β-trefoil proteins, human interleukin-1β (IL-1β)[1] (*10*−*16*) and human basic fibroblast growth factor (bFGF) (*17*, *18*). IL-1β is a cytokine, while bFGF is a growth factor; thus, the functions of these proteins are unrelated to that of hisactophilin. There is no detectable sequence homology between hisactophilin and the other β-trefoil proteins; however, they do all contain medium or large hydrophobic residues at 18 structurally conserved positions (*9*, *19*). Recent experimental and theoretical studies indicate that folding pathways may be conserved among proteins with diverse primary sequences but the same overall fold (*20*). Consequently, it is of great interest to compare the stability and folding of unrelated proteins that adopt the same fold.

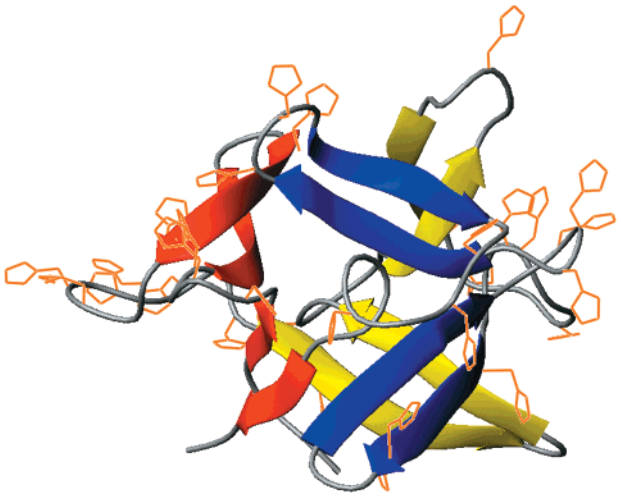

FIGURE 1: Side view of structure of hisactophilin. The β-trefoil structure consists of three trefoil units, each containing four sequential β-strands. The structure is colored to highlight β-hairpins formed by β-strands: 1−12 and 2−3 (red); 4−5 and 6−7 (yellow); 8−9 and 10−11 (blue). The 31 histidine residues are shown in yellow. The first and fourth strands from each trefoil form a six-stranded antiparallel β-barrel, while the second and third strands form a hairpin triplet, which packs against one end of the β-barrel.

[†] This work was supported by the Natural Sciences and Engineering Research Council of Canada.

* To whom correspondence should be addressed. E-mail: meiering@uwaterloo.ca, fax: 1-519-746-0435, phone: 1−519-888-4567.

[1] Abbreviations: CD circular dichroism; DSC, differential scanning calorimetry; DTT, dithiothreitol; EDTA, ethylenediaminetetraacetic acid; MES, *N*-morpholinoethanesulfonic acid; LEM, linear extrapolation method; DBM, denaturant binding model; BEM, binomial extrapolation method; IL-1β, interleukin-1β; bFGF, basic fibroblast growth factor.

10.1021/bi002609i CCC: $20.00
Published on Web 03/09/2001

In this paper, we report characterization of the thermodynamic stability of hisactophilin as a function of pH and temperature, measured by urea denaturation curves, optically monitored thermal denaturation curves, and differential scanning calorimetry (DSC). The data are interpreted in terms of the function of hisactophilin and in terms of the β-trefoil superfold.

EXPERIMENTAL PROCEDURES

Protein Expression and Purification. Recombinant hisactophilin was obtained as described previously (*7*). Purified hisactophilin was dialyzed against 10 mM ammonium carbonate solution (pH 7.9), lyophilized, and stored at −20 °C.

Solution Preparation. Stock buffer solutions were prepared gravimetrically by weighing out appropriate quantities of conjugate acid and conjugate base (MES/NaMES for pH 5.6−6.2; KH_2PO_4/K_2HPO_4 for pH 5.7−7.7; and glycine/sodium glycinate for pH 8.7−9.7). Stock urea solutions were made gravimetrically using ultrapure urea (>99.5%, Bio-Shop) and stored frozen at −20 °C. Dilutions of stock solutions were made using Hamilton syringes. Final urea concentrations were confirmed using a refractometer (Bausch & Lomb Optical Co., NY) (*21*).

Urea Denaturation Curves. For urea denaturation curves, a 10× protein solution was prepared by dissolving lyophilized protein to a concentration of 2−3 mg mL^{-1} in 500 mM buffer containing 10 mM DTT and 10 mM EDTA. The protein solution was diluted 10-fold with a combination of urea solution and water to give the final desired urea concentration. Samples were equilibrated for at least 2 h at the appropriate temperature (20.0 or 5.0 °C), before taking readings in the spectrofluorometer (Fluorolog-22, Jobin Yvon-Spex, Instruments S.A., Inc., NJ) or CD spectropolarimeter (J715, Jasco). Temperature control was achieved using a water bath (RTE-211, NESLAB Instruments Inc., NH) for the fluorometer, or by a Peltier cell (ELFIN model ELDC5D4, Japan Servo Co. Ltd.) for the polarimeter. Fluorescence readings were made in 1-cm path-length cuvettes using either the J715 CD spectropolarimeter (fluorescence mode, 280 nm long-pass filter, slit widths 5 nm, scanning excitation spectrum from 260 to 300 nm), or the Fluorolog-22 (with excitation and emission wavelengths and slit widths set to 277 and 306 nm, and 1 and 5 nm, respectively). CD data were acquired at 227 nm using slit widths of 5 nm and a 1-mm path-length cuvette.

Denaturation curve data were fit using the linear extrapolation method (LEM) to a two-state transition between the native and the denatured state, with a nonsloping pretransition baseline and a sloping post-transition baseline according to the following equation:

$$Y = \frac{Y_N - \langle Y_N - (Y_U + S_U[\text{urea}])\rangle \exp\left(\dfrac{-\Delta G_u^{H_2O} + m[\text{urea}]}{RT}\right)}{1 + \exp\left(\dfrac{-\Delta G_u^{H_2O} + m[\text{urea}]}{RT}\right)} \quad (1)$$

where Y is the measured optical signal at a given urea concentration, Y_N is the signal for the native state, which is independent of urea concentration, Y_U is the signal for the unfolded state in the absence of urea, S_U is the urea dependence of the signal for the unfolded state, R is the gas constant, T is the temperature in Kelvin, $\Delta G_u^{H_2O}$ is the Gibbs free energy of unfolding of the protein at temperature T in 0 M urea, and m is the denaturant dependence of ΔG_u (*21*, *22*).

DSC. DSC experiments were performed using a nano differential scanning calorimeter (Calorimetry Sciences Corporation). Protein samples were prepared by dissolving lyophilized hisactophilin in the appropriate buffer, followed by extensive dialysis and centrifugation, and pH measurement of the final solution. Protein concentrations were determined by absorbance at 280 nm, using an extinction coefficient of 0.330 at 280 nm for a 1 mg mL^{-1} hisactophilin solution, as determined using the method of Gill and von Hippel with correction for light scattering (*23*, *24*). DSC samples from pH 5.59 to pH 6.25 typically contained ∼2.5 mg mL^{-1} protein, 50 mM MES/NaMES, 1 mM EDTA, and 1 mM DTT. MES was used because it has high buffering capacity over this pH range where hisactophilin thermal unfolding is highly pH dependent [pK_a of 6.15 at 20.0 °C (*25*)].

DSC samples were degassed just before loading into the DSC cells and scanned under a constant excess pressure of 2.5 atm to prevent bubble formation. Protein samples were routinely rescanned to check reversibility. The shapes of baselines were similar from one experiment to another; however, the offsets varied so that it was not possible to calculate absolute values of C_p. Results were independent of heating rate, except that reversibility decreased at slow scan rates. Samples were therefore routinely scanned at a heating rate of 1 K min^{-1} to the minimum temperature required to obtain an adequate post-transition baseline (i.e., generally to 75−85 °C, depending on pH).

DSC thermograms were analyzed as described elsewhere (*26*) using Microcal Origin software (version 5.0, Microcal Software Inc., USA) to obtain the temperature at the midpoint of the unfolding transition, T_g, and the calorimetric and van't Hoff enthalpy of denaturation. ΔH^{vH} and ΔH^{cal} were found to agree within experimental error, consistent with a two-state equilibrium. ΔH^{vH} was used for further analysis since it has lower experimental error (*27*, *28*).

Optically-Monitored Thermal Denaturation Curves. Samples were prepared as described for urea denaturation curves. CD data collection at pH 5.80 was automated using the Experiment Manager application of the Jasco software. Both the heating and the cooling experiments were started at 20.0 °C, with a 2.0 °C increment and 3 min equilibration time for heating, and 1.0 °C and 4 min for cooling. Longer times were needed at lower temperatures to ensure equilibrium. At the end of heating or cooling, the sample temperature was returned to 20.0 °C to determine reversibility. At pH 5.80, cooling transitions were essentially fully reversible, while the heating transitions were >90% reversible. For fluorescence-monitored experiments at pH 9.7, the water bath was programmed to heat the sample at 1 °C min^{-1}, and the temperature in the cuvette was monitored using a copper−constantan thermocouple. Sample fluorescence was measured continuously during heating, and also after reequilibrating the sample after heating to determine reversibility. The

fluorescence-monitored experiments were much more reversible (~80−100%) than DSC experiments at this pH, due to the use of lower protein concentrations in the fluorescence experiments.

Optically monitored thermal denaturation data at pH 5.80 and 9.7 were analyzed (*29*) by fitting the temperature dependence of the optical signals of the native state and denatured state to straight lines, except for the CD of the native state which was temperature-independent. At each temperature, T, the fraction of the unfolded protein, f_u, was then calculated using:

$$f_u = \frac{Y_{obs} - Y_U}{Y_N - Y_U} \quad (2)$$

where Y_{obs} is the observed CD signal, Y_U is the signal of the unfolded state, and Y_N is the signal of the native state. The equilibrium constant, K_u, at T is given by

$$K_u = \frac{f_u}{1 - f_u} \quad (3)$$

Values of K_u were converted to the corresponding values of Gibbs free energy of unfolding using:

$$\Delta G_u(T,[\text{urea}]) = -RT \ln K_u \quad (4)$$

RESULTS

The thermodynamic stability of hisactophilin was measured using urea denaturation curves, optically monitored thermal denaturation curves and DSC.

Urea Denaturation Curves. For urea-induced unfolding, the structure of hisactophilin was monitored using fluorescence and far-UV CD. Hisactophilin has a relatively low intrinsic fluorescence since it does not contain tryptophan. Fluorescence therefore arises mainly from three tyrosine residues: Tyr62 is exposed to solvent on the surface of the protein, while Tyr52 and Tyr92 are partially buried near the protein surface (*8*). The fluorescence spectrum has an emission maximum at 306 nm both in the absence and in the presence of urea, and the fluorescence intensity increases with increasing urea concentration (Figure 2, panel A). The far-UV CD signal of native hisactophilin is also relatively weak, as is generally observed for all-β proteins. In the absence of denaturant, the CD spectrum of hisactophilin has broad minima at 209 and 200 nm, and a maximum at 227 nm (Figure 2, panel B). The minimum at 209 nm is typical for β-sheet structure, while the minimum at 200 nm has been observed in class II β-proteins and unstructured proteins (*30*). The maximum at 227 nm is a combination of contributions from secondary structure, including the many β-turns and loops in the protein, and from aromatic residues (*31*, *32*). The CD spectrum of recombinant hisactophilin is very similar to that of natural hisactophilin, which contains an N-terminal myristoyl group (*3*). Thus, the myristoyl group does not appear to have a major effect on the secondary structure of the protein. The hisactophilin CD spectrum has some similarities to that of IL-1β, which is also a relatively weak spectrum consistent with a large proportion of β-structure (*10*). At high urea concentration, the CD spectrum of hisactophilin is typical of unstructured protein (*30*).

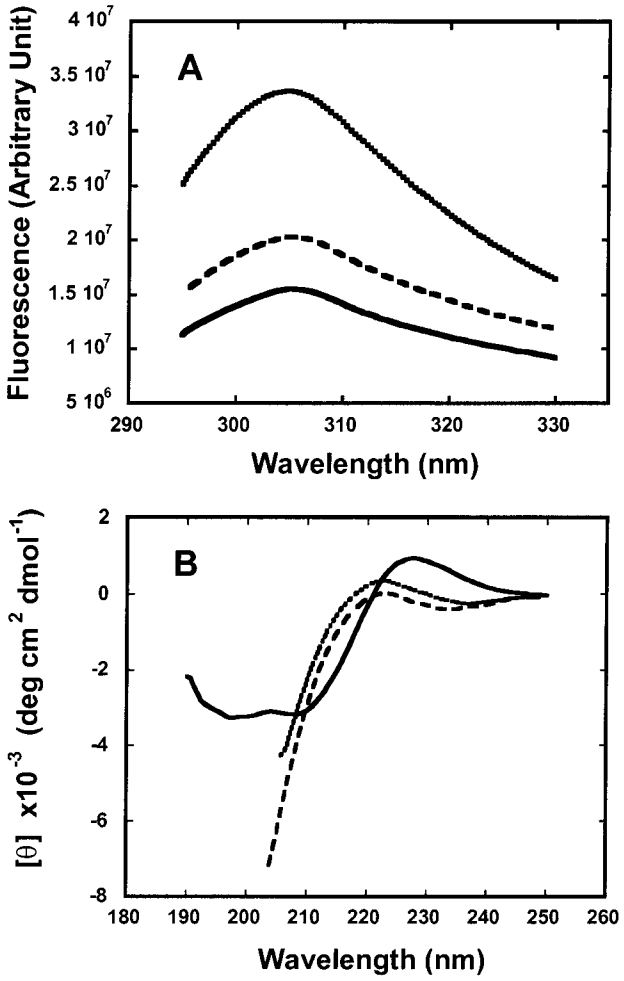

FIGURE 2: (A) Fluorescence and (B) far-UV CD spectra of hisactophilin. Spectra were obtained at 20.0 °C, pH 5.7 (50 mM KH_2PO_4/K_2HPO_4 buffer with 1 mM EDTA and 1 mM DTT, protein concentration 0.24 mg mL^{-1} for fluorescence and 2.3 mg mL^{-1} for CD) in 0 M (solid line), 3.0 M urea (dashed line), and 8.0 M urea (dotted line). Fluorescence spectra were acquired in a 1-cm cuvette using an excitation wavelength of 277 nm, with excitation and emission slit widths set to 1 nm, and 5 nm, respectively. CD spectra were recorded with a 0.01-cm path length cell and a 2-nm bandwidth. CD spectra are an average of 10 scans with the baseline subtracted.

The fluorescence and CD spectra change little from pH 5.7 to pH 9.7, at any given urea concentration. This is consistent with NMR studies on hisactophilin as a function of pH (*7*), which found that the overall structure of the protein is maintained over this pH range. In the absence of denaturant, the spectra do change dramatically below pH ~5.5 and above pH 11.4, as the protein begins to unfold at extreme pH values (data not shown).

Fluorescence- and CD-monitored urea denaturation curves of hisactophilin (Figure 3) were acquired at 20.0 °C from pH 5.7 to pH 9.7 (Table 1). The reversibility of urea-induced unfolding is >90% at all pH values, and the results are independent of protein concentration from ~0.2−2.5 mg mL^{-1}. At a given pH and temperature, data can be fit using eq 1 for a two-state transition, and results obtained by fluorescence and CD agree within experimental error, consistent with a two-state model for unfolding (Figure 3 and Table 1). At 20.0 °C, hisactophilin stability is relatively constant from pH 7.7 to pH 9.7, but it decreases markedly from pH 7.7 to pH 5.7 (Figure 4). Stability also decreases

Table 1: Urea Denaturation Curve Analysis of Hisactophilin Stability[a]

				linear extrapolation method[e]			binomial extrapolation method[e]		
pH	temp (°C)	probe	buffer[b]	m (kcal mol^{-1} M^{-1})	C_{mid} (M)	$\Delta G_u^{H_2O}$ (kcal mol^{-1})	m_1 (kcal mol^{-1} M^{-1})	C_{mid} (M)	$\Delta G_u^{H_2O}$ (kcal mol^{-1})
5.70	20.0	CD	KPi	2.24 ± 0.17	1.02 ± 0.02	2.28 ± 0.19	2.29 ± 0.10	1.02 ± 0.01	2.27 ± 0.11
	20.0	CD	MES	2.19 ± 0.12	1.05 ± 0.02	2.20 ± 0.13	2.35 ± 0.12	1.05 ± 0.02	2.39 ± 0.12
	20.0	Fl	KPi	2.19 ± 0.20	1.06 ± 0.03	2.32 ± 0.22	2.37 ± 0.20	1.06 ± 0.03	2.42 ± 0.22
	20.0	Fl	MES	2.20 ± 0.19	0.99 ± 0.03	2.18 ± 0.21	2.36 ± 0.19	1.00 ± 0.03	2.28 ± 0.21
5.87[d]	5.0	CD	MES	1.90 ± 0.09	0.91 ± 0.02	1.73 ± 0.09	2.05 ± 0.09	0.92 ± 0.01	1.82 ± 0.09
6.20[c]	20.0	Fl	MES	2.39 ± 0.15	2.23 ± 0.02	5.33 ± 0.31	2.68 ± 0.15	2.23 ± 0.03	5.63 ± 0.31
	20.0	Fl	MES + 400 mM NaCl	2.56 ± 0.14	1.39 ± 0.02	3.56 ± 0.19	2.85 ± 0.14	1.40 ± 0.02	3.84 ± 0.19
6.70	20.0	CD	KPi	1.63 ± 0.18	3.10 ± 0.05	5.04 ± 0.48	2.15 ± 0.14	3.26 ± 0.04	6.25 ± 0.44
	20.0	Fl	KPi	1.62 ± 0.14	3.08 ± 0.04	5.10 ± 0.38	1.96 ± 0.26	3.15 ± 0.09	5.46 ± 0.79
7.08[d]	5.0	Fl	KPi	1.67 ± 0.16	2.00 ± 0.04	3.34 ± 0.32	1.96 ± 0.16	2.00 ± 0.04	3.64 ± 0.32
7.70	20.0	CD	KPi	1.63 ± 0.05	4.31 ± 0.01	7.11 ± 0.73	2.23 ± 0.06	4.31 ± 0.02	8.30 ± 0.23
	20.0	Fl	KPi	1.59 ± 0.22	4.26 ± 0.10	6.78 ± 0.94	2.13 ± 0.05	4.39 ± 0.02	7.96 ± 0.19
8.15	20.0	Fl	KPi	1.65 ± 0.08	4.61 ± 0.16	7.59 ± 0.37	2.22 ± 0.07	4.62 ± 0.02	8.71 ± 0.33
8.70	20.0	CD	Gly	1.46 ± 0.04	5.18 ± 0.03	7.55 ± 0.19	2.14 ± 0.06	5.21 ± 0.04	9.21 ± 0.27
	20.0	Fl	Gly	1.49 ± 0.06	5.19 ± 0.03	7.75 ± 0.20	2.28 ± 0.07	5.33 ± 0.33	10.11 ± 0.34
	20.0	Fl	Gly + 400 mM NaCl	1.47 ± 0.13	4.53 ± 0.04	6.64 ± 0.55	2.11 ± 0.12	4.55 ± 0.05	8.11 ± 0.53
9.70	20.0	CD	Gly	1.53 ± 0.07	4.58 ± 0.02	7.03 ± 0.25	2.17 ± 0.07	4.59 ± 0.02	8.45 ± 0.31
	20.0	Fl	Gly	1.65 ± 0.15	4.76 ± 0.04	7.85 ± 0.62	2.04 ± 0.10	4.84 ± 0.08	8.17 ± 0.42

[a] Error estimates are from fitting data to eq 1 using nonlinear least squares regression analysis by the program KaleidaGraph (Synergy Software). Solution conditions were 0.2−0.3 mg mL^{-1} protein in 50 mM buffer containing 1 mM EDTA and 1 mM DTT. [b] KPi is KH_2PO_4/K_2HPO_4 and Gly is glycine/sodium glycinate. [c] Denaturation curve in MES at pH 5.7 + 400 mM NaCl was also acquired but data could not be fit accurately as C_{mid} was significantly decreased. [d] These pH values are adjusted for the temperature under which the denaturation curves were obtained using $dpK_a/dT = -0.025$ for KPi (*55*) and −0.011 for MES (*25*). [e] For linear extrapolation method (LEM) the equilibrium m was fit as a constant in eq 1, while for the binomial extrapolation method (BEM), m_2 was fixed to 0.072 based on fit of data in Figure 8 and m_1 was fit as a constant in eq 14.

when temperature is decreased from 20.0 to 5.0 °C at pH 5.7 and 6.7 (Table 1).

Thermal Stability of Hisactophilin. The stability of hisactophilin as a function of temperature was investigated further using DSC and optically monitored thermal denaturation curves. The equations used to describe the thermodynamics of protein stability in terms of a reversible two-state transition between the folded and denatured states are given below (*29*):

$$\Delta H(T) = \Delta H_{T_g} + \Delta C_p(T - T_g) \quad (5)$$

$$\Delta S(T) = \Delta S_{T_g} + \Delta C_p \ln\left(\frac{T}{T_g}\right) \quad (6)$$

$$\Delta G(T) = \Delta H(T) - T\Delta S(T) \quad (7)$$

$$\Delta G(T) = \Delta H_{T_g}\left(1 - \frac{T}{T_g}\right) + \Delta C_p\left[T - T_g - T\ln\left(\frac{T}{T_g}\right)\right] \quad (8)$$

where $\Delta H(T)$ is the enthalpy of unfolding at temperature, T, ΔH_{T_g} is the unfolding enthalpy at the midpoint of the heat unfolding transition, T_g, $\Delta S(T)$ is the entropy of unfolding at a given temperature, ΔS_{T_g} is the entropy of unfolding at T_g, $\Delta G(T)$ is the Gibbs free energy of unfolding at T, and ΔC_p is the difference in heat capacity between the folded and unfolded state of the protein. All the Δ values correspond to the value for the unfolded state relative to the value for the native state.

Equation 8 describes a pseudo-parabolic temperature dependence for $\Delta G(T)$. Thus, a protein will have a temperature at which it has maximum stability and stability decreases above and below this temperature. A protein may therefore undergo both a heat-induced unfolding transition, with a midpoint, T_g, and a cold-induced unfolding transition, with a midpoint T_g'. Heat unfolding generally occurs below 100 °C and so is easily measurable experimentally. In contrast, cold unfolding generally occurs below 0 °C under most solution conditions and so is not easily measurable. Cold unfolding may be observed, however, by destabilizing a protein using low pH or by adding denaturants such as urea (*33*).

DSC. DSC experiments on hisactophilin were performed from pH 5.4 to pH 9.7. At all pHs a single endotherm, corresponding to high temperature-induced protein unfolding, was observed as temperature was increased from 0 to 70−80 °C. Reversibility was at least 80% and generally >90% below pH 6.25 (Figure 5). At pH 6.7, reversibility was only ∼2%, at pH 7.7 it was ∼20%, and at pH 8.7 and pH 9.7 it was ∼45%. Since hisactophilin has a pI of ∼6.9 (*1*), the decreased reversibility is likely related to the decreased net charge of the protein at increased pH and high temperature, as has been observed for other proteins (*27*). The use of higher protein concentrations for DSC experiments may also decrease the reversibility relative to urea-induced denaturation. There was some evidence for a second unfolding transition in DSC thermograms at low pHs, corresponding to low temperature-induced unfolding near 0 °C. This transition was difficult to measure, however, due to the low quality of the DSC baseline at low temperature, and potential problems with freezing the protein solution. Cold unfolding was therefore investigated further using optically monitored denaturation curves (vide infra).

The high-temperature unfolding transition from pH 5.4 to pH 6.2 was analyzed in terms of a reversible process (*34*). T_g and ΔH_{T_g} values obtained from the data fitting are summarized in Table 2. Consistent with the results of urea denaturation curves, the DSC data show that hisactophilin stability decreases markedly with decreasing pH, based on decreasing T_g values from pH 6.2 to pH 5.4.

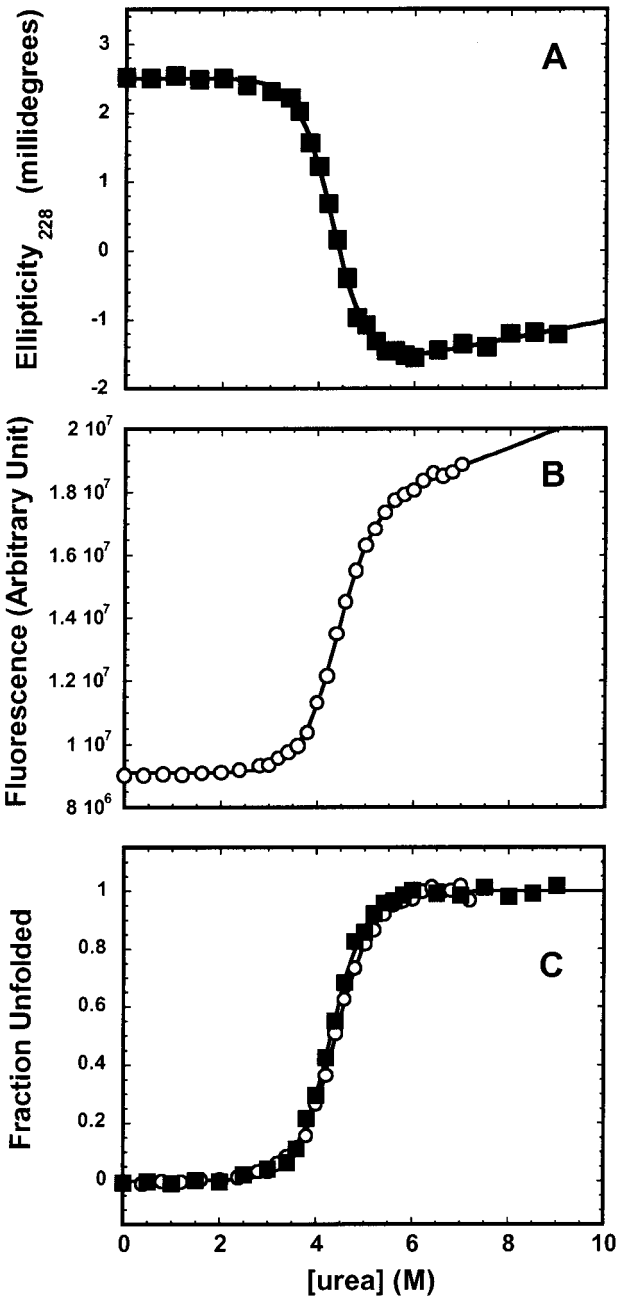

FIGURE 3: Optically monitored urea denaturation curves at pH 7.7. Solutions contained 50 mM KH_2PO_4/K_2HPO_4, pH 7.7, 1 mM EDTA, 1 mM DTT, and 0.2 mg mL^{-1} protein at 20.0 °C. (A) CD (■), (B) fluorescence (○), (C) fraction of unfolded protein as measured by CD (■) and fluorescence (○) are coincident, consistent with a two-state unfolding transition.

$\Delta G(T)$ values can be calculated from DSC data using eq 8. To do this, the change in heat capacity upon unfolding, ΔC_p must be known. ΔC_p is defined from the Kirchoff equation as:

$$\Delta C_p = \left(\frac{d\Delta H_{T_g}}{dT}\right) \qquad (9)$$

Equation 9 has been used extensively to give a reliable measure of the ΔC_p for the unfolding of proteins, by measuring ΔH_{T_g} and T_g as a function of pH (*34*). Using the DSC data from pH 5.4 to pH 6.2, a linear regression analysis of ΔH_{T_g} versus T_g yields a value of ΔC_p of 2.4 ± 0.3 kcal mol^{-1} K^{-1} for hisactophilin. This value was used to calculate values for $\Delta G_u(293)$ corresponding to the different pHs at T_g, pH_{T_g} (Table 2). The DSC values for $\Delta G_u(293)$ at pH_{T_g} ~5.7 are somewhat higher than the values obtained by urea denaturation at the same pH. This is probably because pH_{T_g} is underestimated in DSC samples, due to the buffering action of the histidines of hisactophilin (~5.6 mM histidine for 2.5 mg mL^{-1} protein solution for DSC, as compared with ~0.56 mM for urea denaturation) and due to nonlinear behavior of ΔG_u in urea (vide infra). Since the stability is so strongly pH-dependent, only a small difference in pH can account for the differences between the DSC and urea denaturation results.

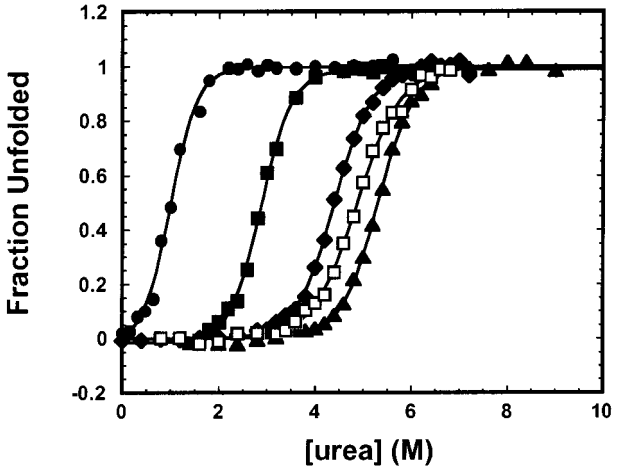

FIGURE 4: Fluorescence-monitored urea denaturation curves for pH 5.7 (●), pH 6.7 (■), pH 7.7 (◆), pH 8.7 (▲), and pH 9.7 (□), displayed in terms of the fraction of unfolded protein. Solutions contained 50 mM buffer (KH_2PO_4/K_2HPO_4 buffer and MES/NaMES for pH 5.7, KH_2PO_4/K_2HPO_4 buffer for pH 6.7 and 7.7, glycine/sodium glycinate for pH 8.7 and 9.7), 1 mM EDTA, 1 mM DTT, and 0.2−0.3 mg mL^{-1} protein, at 20.0 °C. Hisactophilin stability increases markedly from pH 5.7 to pH 7.7 and then remains relatively constant from pH 7.7 to pH 9.7.

Table 2: DSC Analysis of Hisactophilin Stability

pH_{293K}	pH_{T_g}[a]	T_g (°C)	ΔH_{T_g} (kcal mol^{-1})	$\Delta G_u(293,0)$ (kcal mol^{-1})	$\Delta\nu$
5.59	5.32	47.0	51.4	1.5	3.4
5.75	5.45	48.9	51.7	1.4	3.4
5.81	5.46	53.6	62.9	2.1	4.0
6.03	5.63	58.3	73.1	2.8	4.5
6.09	5.69	58.7	84.4	4.1	5.2
6.25	5.81	61.7	83.9	3.8	5.1

[a] pH corrected to value at T_g using $dpK_a/dT = -0.011$ for MES (*25*). Errors in each point are about ± 10% for ΔH_{T_g} and ± 0.4 °C for T_g. A linear regression fit of ΔH_{T_g} versus T_g gives a ΔC_p value (eq 9) of 2.4 ± 0.3 kcal mol^{-1} K^{-1}.

The pH-dependent DSC data can be used to calculate the number of protons released upon unfolding, using eq 10 (*34*):

$$\Delta\nu = \nu_U - \nu_N = \frac{\Delta H_{T_g}}{2.303RT_g^{\,2}}\frac{dT_g}{d\mathrm{pH}} \qquad (10)$$

where ν_U and ν_N are the number of protons bound to the denatured and native states, and $\Delta\nu$ is the number of protons associated with protein unfolding. Values of $\Delta\nu$ are given in Table 2.

Optically Monitored Thermal Denaturation Curves. (a) pH 5.8. To further investigate the temperature dependence

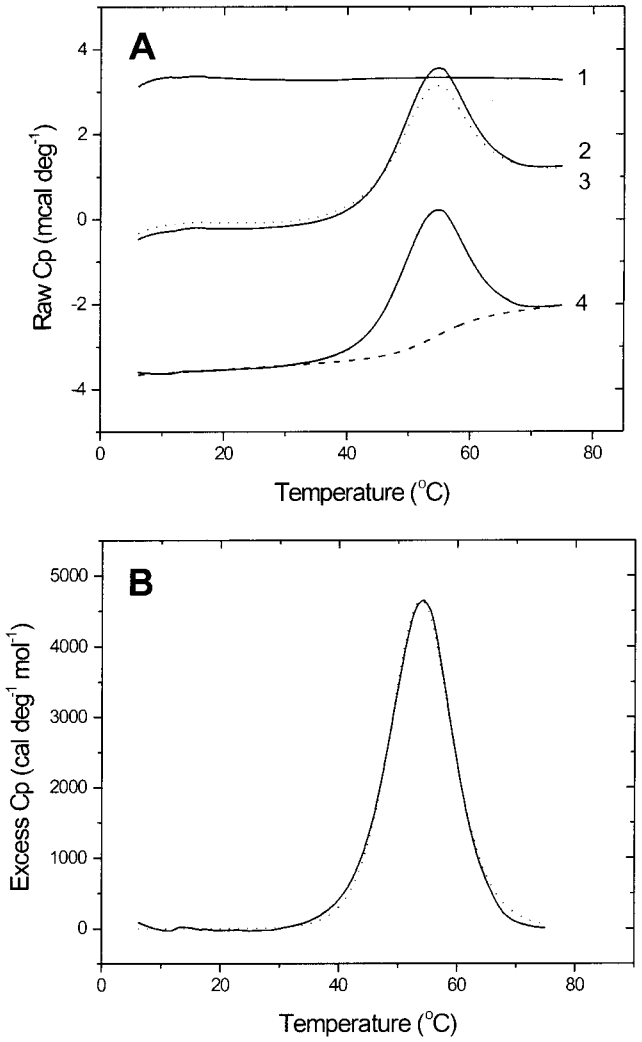

FIGURE 5: Representative DSC thermograms of the denaturation of hisactophilin in 50 mM MES/NaMES, pH 5.83, 1 mM EDTA, 1 mM DTT. (A) Raw data for 1, buffer baseline scan; 2, unfolding endotherm; 3, results of rescanning the sample of endotherm 2; and 4, hisactophilin data corrected for the buffer baseline and indicating the interpolative baseline (dashed line) used to eliminate the denaturation heat capacity changes. (B) Normalized data (solid line) fit to a non-two-state transition model (dotted line). The T_g is 53.9 °C with ΔH^{vH} of 60.8 kcal mol^{-1} and ΔH^{cal} of 64.7 kcal mol^{-1} ($\Delta H^{vH}/\Delta H^{cal} = 0.94$).

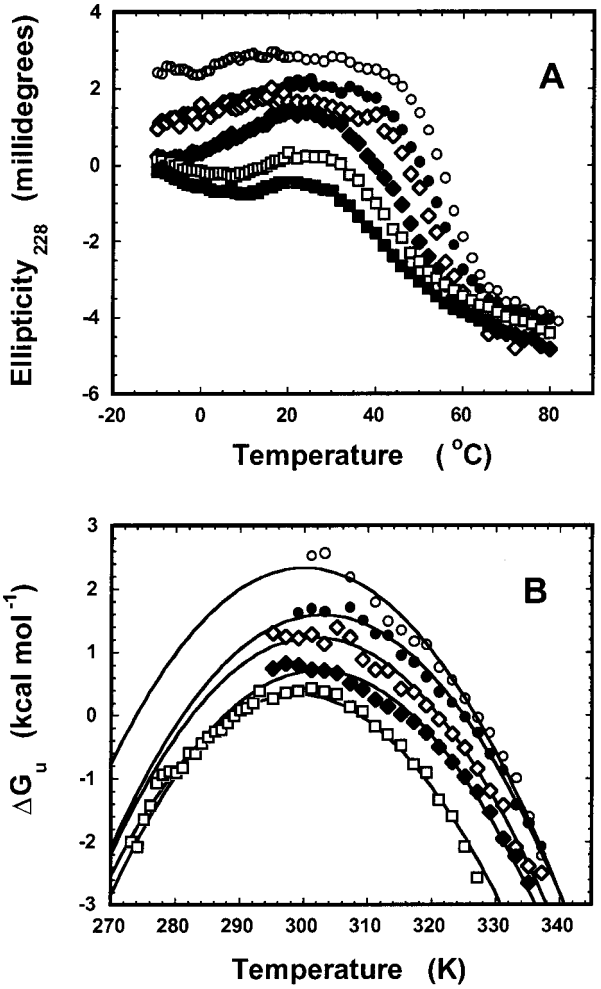

FIGURE 6: Thermal unfolding of hisactophilin at pH 5.80. Unfolding was monitored by CD at 228 nm using a 0.1-cm path-length cuvette. Solutions contained 0.29 mg mL^{-1} protein in 50 mM MES/NaMES, pH 5.80, 1 mM EDTA, 1 mM DTT, and 0−1.25 M urea. (A) CD signal change as a function of temperature for 0.00 M (○), 0.25 M (●), 0.50 M (◇), 0.75 M (◆), 1.00 M (□), and 1.25 M (■). Data are averaged for two separate experiments. "Sigmoidal" decreases in CD signals with increasing and decreasing temperature, followed by sloping baseline regions indicate that hisactophilin is undergoing both high and low-temperature unfolding. (B) Raw data were converted to $\Delta G_u(T,[\text{urea}])$ as described in text. Using $\Delta C_p = 2.0$ kcal mol^{-1} K^{-1} (obtained from van't Hoff plots of the high-temperature unfolding data), $\Delta G_u(T,[\text{urea}])$ values were fit to eq 8. Values from fits are summarized in Table 3. Direct fitting of ΔC_p for data at 1.00 M gives 2.13 ± 0.04 kcal mol^{-1} K^{-1}.

of hisactophilin stability, in particular, cold unfolding, CD-monitored thermal denaturation curves were obtained by heating and by cooling the protein from 20.0 °C in various concentrations of denaturant at pH 5.8 (Figure 6), where the heat-induced unfolding monitored by CD was >95% reversible.

At pH 5.8, both heat and cold unfolding transitions are evident in the CD-monitored curves in the presence of 0 to 1.25 M urea (Figure 6, panel A). The CD signal decreases upon unfolding, for both heat- and cold-induced transitions. The baselines for heat- and cold-unfolded hisactophilin appear to be continuous (Figure 6, panel A). This suggests that the heat- and cold-unfolded states are thermodynamically indistinguishable, as has been found for other proteins (*33*) and is borne out in the following analysis.

Direct fitting of the cold unfolding data is difficult, particularly at low denaturant concentrations, due to the relatively small amplitude of the CD signal changes and poorly defined cold-unfolded baselines. Also, the pH of the samples will change significantly over a large temperature range, and this will complicate the analysis because hisactophilin stability is very sensitive to pH in this range. The data were therefore first analyzed by fitting only the high-temperature unfolding data using van't Hoff analysis (linear ln K_u vs $1/T$ plot) using fraction unfolded from ~0.35−0.65 (pH can reasonably be treated as constant over this relatively small temperature range). Van't Hoff enthalpies, $\Delta H^{vH}_{T_g}$, and melting temperatures, T_g, are summarized in Table 3. The slope of the linear plot of $\Delta H^{vH}_{T_g}$ versus T_g (eq 9) gives an apparent change in heat capacity, ΔC_p^{app}, of 2.0 ± 0.2 kcal mol^{-1} K^{-1}. This gives an estimate of ΔC_p because the analysis does not account for the enthalpic contribution of urea binding to protein (*35*−*38*). Since this ΔC_p^{app} value is very similar to the value of 2.4 ± 0.3 kcal mol^{-1} obtained

Table 3: Analysis of Hisactophilin Thermal Denaturation at pH 5.8 at Different Urea Concentrations[a]

[urea] (M)	T_g^{vH} [b] (°C)	$\Delta H_{T_g}^{vH}$ [b] (kcal mol^{-1})	T_g [c] (°C)	ΔH_{T_g} [c] (kcal mol^{-1})	T'_g [c] (°C)	$\Delta H_{T'_g}$ [c] (kcal mol^{-1})
0.00	53.9	53.9	53.7	56.0	0.8	−49.8
0.25	51.0	45.1	51.9	46.0	8.1	−41.7
0.50	47.4	41.7	48.0	40.2	9.5	−36.9
0.75	42.7	30.4	43.8	30.1	14.6	−28.3
1.00	35.2	19.4	35.7	20.3	15.8	−19.4

[a] Samples contained 0.29 mg mL^{-1} hisactophilin in 50 mM MES/NaMES, 1 mM EDTA, and 1 mM DTT. Sample pH was 5.80 at 20.0 °C, thus based on $dpK_a/dT = -0.011$ for MES (*25*), pH_{T_g} varied from 5.43 for the 0 M sample to 5.63 for the 1.0 M sample. [b] Values of T_g^{vH} and $\Delta H_{T_g}^{vH}$ were obtained by fitting high-temperature unfolding data from Figure 6, panel A, using van't Hoff analysis, as described in Results. [c] Values of T_g, ΔH_{T_g}, and T'_g, $\Delta H_{T'_g}$ were obtained by fitting the high-temperature unfolding data for 0.00 to 0.75 M urea and both high- and low-temperature data for 1.00 M urea to eq 8.

for ΔC_p by calorimetry; however, it seems that urea does not have a large effect on unfolding enthalpies of hisactophilin at the relatively low denaturant concentrations used here.

The thermal unfolding data were also analyzed by directly fitting $\Delta G(T)$ versus T values to eq 8 (*35*−*37*) (Figure 6, panel B). Since the cold unfolding transition is not well defined for 0 to 0.75 M urea, and the pH varies significantly over large temperature ranges, only the heat unfolding data were analyzed for these results. For the 1.00 M data, the cold unfolded baseline is well defined and heat and cold unfolding occur over a narrower temperature range; thus, both branches were analyzed simultaneously. The 1.25 M data cannot be fit in this way because the protein is more than 50% unfolded at all temperatures. In principle, ΔC_p can be fit directly in this analysis; however, the error in this value is very high if only the heat unfolding transition is analyzed. Consequently, for 0 to 0.75 M urea, ΔC_p was fixed to 2.0 kcal mol^{-1} K^{-1}, the value obtained from the van't Hoff analysis above. For the 1.00 M data, ΔC_p was also fit directly. Values of ΔH_{T_g}, T_g, $\Delta H_{T'_g}$ and T'_g obtained for the fits are summarized in Table 3 and fits are shown in Figure 6, panel B. The data for 0 to 0.75 M are well fit using 2.0 kcal mol^{-1} K^{-1} for ΔC_p, and a similar value of ΔC_p (2.13 ± 0.04 kcal mol^{-1} K^{-1}) is obtained for direct fitting of the 1.00 M data. The values of ΔH_{T_g} and T_g obtained by the direct fitting method agree with the values obtained by van't Hoff analysis within experimental error. Also, the values of ΔH_{T_g} and T_g obtained in 0 M urea by CD-monitored thermal denaturation agree with the values obtained by DSC (Table 2). T_g and ΔH_{T_g} values decrease and T'_g and $\Delta H_{T'_g}$ values increase as the concentration of urea increases, as has been observed for other proteins (*33*).

(b) pH 9.7. Thermal denaturation curves were acquired in the presence of 0 to 2.5 M urea at pH 9.7, using fluorescence to monitor unfolding (Figure 7). Cold-induced unfolding cannot be observed under these conditions, since T'_g is shifted to lower temperatures relative to pH 5.7, due to the increased stability of the protein at pH 9.7 (vide infra and Table 4). The fluorescence-monitored thermal unfolding experiments were much more reversible than DSC experiments at this pH, due to use of lower protein concentrations in the fluorescence experiments.

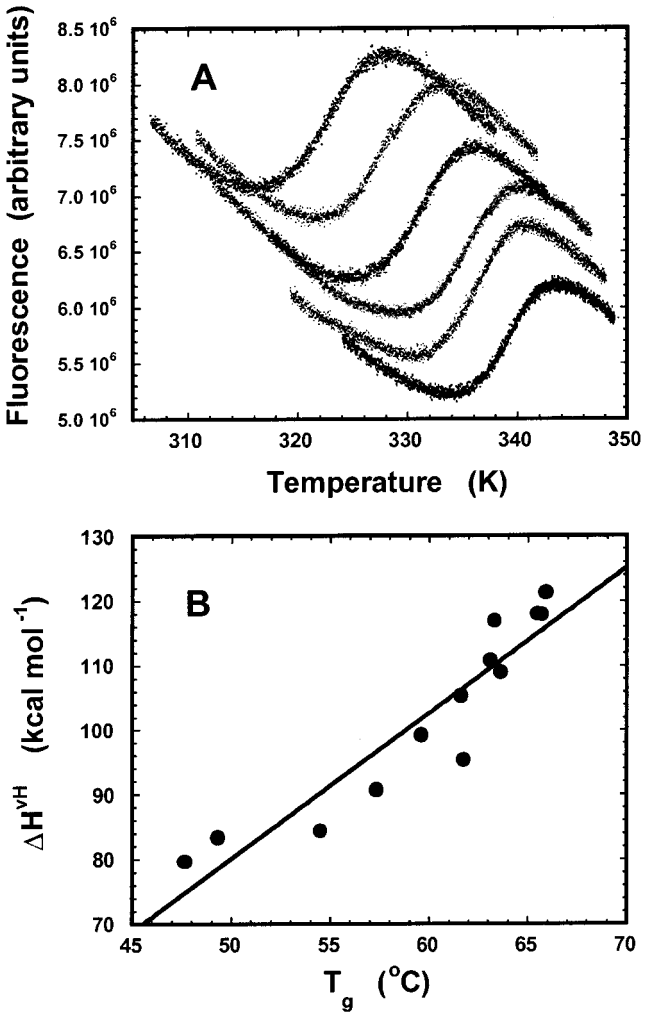

FIGURE 7: Thermal unfolding of hisactophilin at pH 9.7. Unfolding was monitored by fluorescence with excitation and emission wavelengths of 277 and 306 nm, respectively, using a 1-cm path-length cuvette. Solutions contained 0.20 mg mL^{-1} protein in 50 mM glycine/sodium glycinate buffer, pH 9.7, 1 mM EDTA, 1 mM DTT and 0−2.50 M urea. (A) Representative thermal unfolding transitions for (from right to left) 0.00, 0.50, 1.00, 1.50, 2.00, and 2.50 M urea. (B) van't Hoff plot corresponding to data from panel A (each point represents a single thermal denaturation experiment). The estimated errors are about ± 10% for $\Delta H_{T_g}^{vH}$ and ± 1 °C for T_g.

The thermal unfolding data were analyzed using linear van't Hoff analysis as at pH 5.8 (Table 4). A plot of the ΔH_{T_g} versus T_g data in urea at pH 9.7 (Figure 7) gives a value for ΔC_p^{app} of 2.2 ± 0.3 kcal mol^{-1} K^{-1}. This value agrees within error with the value of ΔC_p^{app} obtained for CD-monitored thermal denaturations in urea at pH 5.8, and with the value of ΔC_p obtained by DSC. This confirms that urea does not have a large effect on ΔC_p^{app} relative to ΔC_p and indicates that ΔC_p varies little with temperature for hisactophilin over the range of T_g values investigated (35−66 °C). ΔC_p was therefore again treated as a constant, and an average value of 2.2 kcal mol^{-1} K^{-1} was used to calculate ΔG_u(293,[urea]), $\Delta H_{T'_g}$ and T'_g for the different urea concentrations (Table 4). As expected, cold unfolding is calculated to occur at lower temperature at this pH as compared to pH 5.8.

In Figure 8, the values of ΔG_u(293,[urea]) from thermal denaturation (Table 4) are compared with those from urea

Table 4: Analysis of Hisactophilin Thermal Denaturation at pH 9.7 at Different Urea Concentrations

[urea] (M)	T_g^{vH} (°C)	$\Delta H_{T_g}^{vH}$ (kcal/mol)	T'_g (°C)	$\Delta H_{T'_g}$ (kcal/mol)	pH_{T_g}[a]	$\Delta G_u(293,[urea])$[b] (kcal/mol)
0.00 (3)[c]	65.7	119	−31.6	−95.0	8.56	8.96
0.25	63.3	117	−32.5	−93.6	8.62	8.64
0.50 (2)[c]	63.4	110	−27.2	−89.2	8.61	7.73
0.75	61.6	105	−25.2	−86.0	8.66	7.15
1.00 (2)[c]	60.7	97.2	−20.3	−80.8	8.68	6.16
1.50	57.3	90.7	−18.6	−76.2	8.77	5.42
2.00	54.5	84.3	−16.4	−71.7	8.84	4.73
2.50 (2)[c]	48.5	81.5	−20.2	−69.5	8.99	4.36

[a] Solutions contained 50 mM glycine/sodium glycinate, pH 9.7, at 20.0 °C. The corrected pH at T_g was calculated using temperature coefficient, dpK_a/dT, of −0.025 for Gly (*55*). [b] $\Delta G_u(293,[urea])$ was calculated using average ΔC_p of 2.2 kcal mol^{-1}. [c] Values at 0, 0.50, 1.00, and 2.50 M represent average of 3, 2, 2, and 2 separate experiments, respectively.

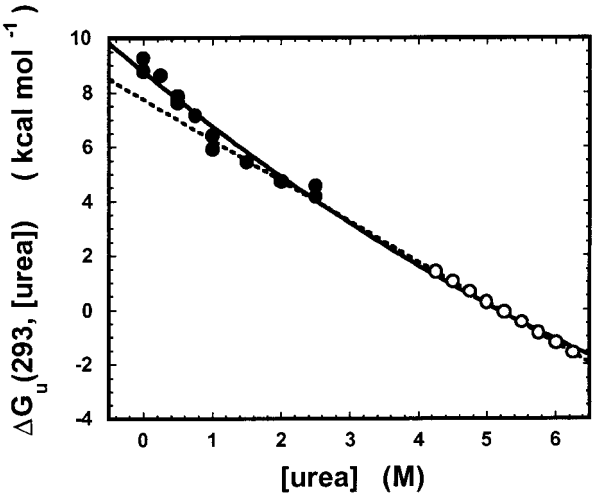

FIGURE 8: Combined $\Delta G_u(293,[urea])$ data from urea denaturation and thermal denaturation. $\Delta G_u(293,[urea])$ values from fluorescence-monitored thermal denaturations in 0−2.50 M urea at pH 9.7 have pH_{T_g} values corresponding to ∼pH 8.7 and so they are combined with urea equilibrium denaturation curve data at pH 8.7. Values of $\Delta G_u(293,[urea])$ from thermal denaturation curves (●) were calculated using eq 8 with $\Delta C_p = 2.2$ kcal mol^{-1} as described in text. Values of $\Delta G_u(293,[urea])$ from urea equilibrium unfolding (○) were calculated from $C_{mid} = 5.19$ M for a distance of ± 1.0 M at intervals of 0.25 M and $m = 1.49$ kcal mol^{-1} M^{-1} for fluorescence denaturation curve at pH 8.7 (Table 1). The fit of combined data to a second-order polynomial according to BEM (eq 11) gives $\Delta G_u(293,[urea]) = 8.76 \pm 0.13 - (2.12 \pm 0.13 \times [urea]) + (0.072 \pm 0.022 \times [urea]^2)$ and is shown by the solid line. Linear extrapolation using only the equilibrium urea denaturation curve data is shown by the dashed line.

denaturation curves (Table 1), taking into account the effect of temperature on solution pH. The $\Delta G_u(293,[urea])$ values from the thermal denaturation data are clearly slightly higher than expected based on linear extrapolation of the transition region data of the equilibrium denaturation curve. This suggests that $\Delta G_u(T,[urea])$ has a nonlinear dependence on urea concentration at low denaturant concentrations. Consistent with this, m values of urea denaturation curves increase with decreasing C_{mid} as pH decreases (Table 1, and Wong, H. J., and Meiering, E. M., unpublished data). Increased m values at low pH have been observed for other proteins and have been attributed to an increased solvent exposure of the denatured state at low pH due to increased electrostatic repulsions (*39*−*41*). To investigate further, equilibrium denaturation curves were acquired at pH 5.7, 6.2, and 8.7 in the presence of NaCl (Table 1). In principle, NaCl should screen the electrostatic repulsions in the unfolded state, leading to a decrease in m value. For hisactophilin, m was unaffected by NaCl, thus, the increase in m with decreasing C_{mid} does not appear to be the result of increased electrostatic repulsions.

Nonlinearity of $\Delta G_u(T,[urea])$ at low denaturant concentrations has been analyzed using binomial extrapolation model (BEM) (*28*, *42*) and denaturant binding model (DBM) (*21*, *22*). The combined data from thermal denaturation and equilibrium urea denaturation in Figure 8 were fit to the equation for BEM:

$$\Delta G_u(T,[urea]) = \Delta G_u(T,0) + m_1[urea] - m_2[urea]^2 \quad (11)$$

where $\Delta G_u(T,[urea])$ is the Gibbs free energy of unfolding at temperature T at any urea concentration, $\Delta G_u(T,0)$ is the Gibbs free energy of unfolding in 0 M urea, m_1 and m_2 are constants. According to this fit (Figure 8), $\Delta G_u(293,[urea]) = 8.73 \pm 0.15 - (2.05 \pm 0.13 \times [urea]) + (0.072 \pm 0.022 \times [urea]^2)$. The data were also fit to the equation for DBM:

$$\Delta G_u(T,[urea]) = \Delta G_u(T,0) - \Delta nRT \ln(1 + aK_{ass}) \quad (12)$$

where Δn is the number of urea molecules binding upon unfolding, a is the denaturant activity, and K_{ass} is the average association constant at each urea binding site. Fitting of these data gave $\Delta G_u(T,0)$ of 8.89 ± 0.15 kcal mol^{-1}, $\Delta n = 29 \pm 7$, and $K_{ass} = 0.144 \pm 0.045$. Fixing K_{ass} to a value of 0.09 as suggested by Filimonov et al. (*42*) gives $\Delta G_u(T,0) = 8.75 \pm 0.10$ and $\Delta n = 42.4 \pm 0.7$. Although the DBM fit agrees well with the experimental data, the values of Δn are lower than might be expected for a protein of this size and amino acid composition (*21*), and the fitted values have rather large errors. Also, direct fits of denaturation curve data to DBM allowing for post transition sloping baseline did not converge, because Δn spiraled downward while K_{ass} spiraled up. Consequently, for hisactophilin the DBM results do not appear to be very reliable.

DISCUSSION

pH-Dependence of Hisactophilin Stability. The pH-dependence of the thermodynamic stability of hisactophilin is rather unusual in that, although the protein is relatively stable from pH 7.7 to pH 9.7, below pH 7.7 stability decreases markedly, and the protein is acid unfolded at a relatively high pH of ∼5. This pH dependence is most likely related to the unusually high proportion of histidine residues in this protein (31 of 118 residues) (*1*). The histidines are located primarily on the surface of the protein (Figure 1) (*8*), and have pK_a values on average close to 6.8 (*7*). Thus, as pH decreases below 7.7, the net charge on hisactophilin increases dramatically as many histidine residues become protonated (*3*). Other ionizable groups in hisactophilin include the side chains of 13 Asp and Glu, and 10 Lys and Arg. Thus, by pH ∼5 the histidines should for the most part be fully protonated, and the net charge on the protein will be in excess of +28. Strong electrostatic repulsion between the many positively charged groups may then cause the protein to unfold.

The function of hisactophilin is also pH-dependent. Measurements of hisactophilin binding to model membranes have revealed that strong binding occurs at pH 6.0, and that binding is essentially abolished as the pH is raised to 7.0 (*3*). Also, based on in vitro experiments, actin binding by hisactophilin is strong at pH 6.5, and negligible at pH 7.5 (*1*). The changes in binding occur over a pH range where histidine ionization occurs (*7*), suggesting that interactions between the positively charged histidines and negative groups of actin and membranes are important for binding. It is interesting that the stability of free hisactophilin is decreased at low pH as the protein becomes positively charged to carry out its biological binding functions. Analogous electrostatic destabilization of a protein due to functional binding requirements has been observed previously for barnase (*43*); it may be a common phenomenon in proteins that bind molecules with high net charge.

From pH 7.7 to pH 9.7, hisactophilin is relatively stable, and stability varies little with pH. In this pH range, hisactophilin has moderate stability as compared to other single domain proteins (*44*). Near physiological pH, the stability of hisactophilin is similar to that of other β-trefoil proteins under comparable conditions, IL-1β [$\sim$7 kcal mol^{-1} (*10*, *45*)] and human bFGF [$\sim$5 kcal mol^{-1} (*17*)].

Cold Unfolding of Hisactophilin. Urea denaturation curves reveal that hisactophilin is clearly destabilized at 5.0 °C as compared to 20.0 °C (Table 1) and appears to undergo cold unfolding even in the absence of denaturant at pH 5.8. While cold unfolding can be observed for many proteins when they are destabilized by adding relatively high concentrations of denaturant, generally it is not observed in the absence of denaturant because T_g' tends to be well below 0 °C (*33*). For proteins with particularly high ΔC_p and low measured experimental enthalpy, ΔH^{exp}, however, cold unfolding will occur at higher temperatures and may be observed in the absence of denaturant (*33*). Hisactophilin meets both of the required thermodynamic characteristics for cold unfolding. It is a relatively large single domain protein with a large hydrophobic core (*19*), and so it has a relatively large ΔC_p (*46*). Consistent with this, the *m* value for hisactophilin is also comparatively large (*47*). In addition, at low pH, ΔH^{exp} is relatively low for hisactophilin as compared to other proteins (*46*).

The low ΔH^{exp} for hisactophilin is likely related to the high histidine content of this protein. ΔH^{exp} is the sum of the enthalpy of the protein conformational change, ΔH_{pr}^{conf}, and the enthalpy of ionization of protein and buffer, ΔH^{ion} (*33*):

$$\Delta H^{exp} = \Delta H_{pr}^{conf} + \Delta H^{ion} = \Delta H_{pr}^{conf} + \sum_i \Delta H_{pr,i}^{ion} + \Delta\nu \Delta H_{buf}^{ion} \quad (13)$$

where $\Delta\nu$ is the number of groups ionized at the protein transition, $\Delta H_{pr,i}^{ion}$ and ΔH_{buf}^{ion}, are the enthalpies of protonation of a single group on the protein and of the buffer, respectively. From analysis using eq 10 (Table 2), the number of protons taken up upon denaturation of hisactophilin ranges from $\sim$3 at pH 5.6 to $\sim$5 at pH 6.2. These values are comparable to values obtained at low pH for other proteins, e.g., $\sim$4−6 for myoglobin (*48*) and $\sim$3 for RNaseA and lysozyme (*49*).

For myoglobin the uptake of protons upon unfolding was attributed to ionization of 5−6 histidine residues, which are buried and neutral in the native state and charged in the unfolded state. For hisactophilin, unfolding may also be accompanied by uptake of protons by histidines, since at least some of these are likely to have a higher pK_a in the unfolded state, which may more readily accommodate a higher net charge than the native state due to its more extended structure. Assuming that the pK_a values of histidines in native hisactophilin are on average $\sim$6.8 (*7*), if the pK_a values for histidines in the unfolded protein are on average $\sim$7.1 (which is in the range observed for random coil proteins), then one would expect a total uptake of $\sim$3 protons by 31 histidine residues at pH 6.2, and an uptake of $\sim$1 proton at pH 5.6, i.e., one expects a decrease in $\Delta\nu$ with decreasing pH. Clearly these calculations are very rough, since they do not take into account the possibility for larger changes in pK_a for individual histidines or proton uptake by other groups such as aspartate. Nevertheless, the calculated trend in $\Delta\nu$ with pH is consistent with the experimental data and suggests that ionization of histidine residues is involved in the proton uptake associated with unfolding.

The enthalpy of ionization of histidines upon unfolding (6.9 kcal mol^{-1}) will be partially offset by ionization of buffer (3.5 kcal mol^{-1} for MES). Assuming that the number of moles of buffer that ionize is equal to the number of moles of histidine that ionize, then the net effect of ionization will be to decrease ΔH^{exp} by $\sim$10 to 17 kcal mol^{-1} for pH 5.6−6.2. This is consistent with the observation that ΔH^{exp} values for hisactophilin are relatively low as compared to values obtained for other proteins (*13*). Interestingly, low values of ΔH^{exp} for myoglobin were also attributed to ionization of histidine residues upon unfolding. Furthermore, cold unfolding was also observed in the absence of denaturant for myoglobin (*48*).

Analysis of Thermal Unfolding and Equilibrium Denaturation Curve Data. For hisactophilin, ΔC_p^{app} measured in urea is very similar to ΔC_p measured by DSC. Comparing with results for other proteins, the effect of denaturant on ΔC_p^{app} is variable; no clear trends are observed for some proteins (*50*−*52*), while for others ΔC_p^{app} decreases slightly (*53*) or increases (*28*) in denaturant. Thus, the effects of denaturant may be protein-dependent. On the basis of the data of Makhadatze and Privalov (*38*), the effects for urea should generally be small, $\sim$0.06 kcal mol^{-1} K^{-1} per molar urea.

The data obtained here indicate that ΔC_p varies little with temperature for hisactophilin, and the thermodynamic data are well fit using a constant value of ΔC_p. Similar results have been obtained for many other proteins (*28*, *35*−*37*, *50*). These results are consistent with other experimental data, which suggest that the temperature-dependence of ΔC_p follows a broad bell-shaped function with a maximum around 40 °C (*46*). For such a function, over moderate temperature ranges in the vicinity of the maximum, ΔC_p can be treated as constant.

Comparison of urea denaturation curve data with thermal denaturation data at high pH suggests that the denaturant dependence of $\Delta G_u(T,[\text{urea}])$ increases at low urea concentrations (Table 4 and Figure 8). In agreement with this, *m* values increase with decreasing C_{mid} at low pH, and this

increase in m value is not affected by increasing ionic strength (Table 1, and Wong, H. J., and Meiering, E. M., unpublished data). Kinetic experiments of hisactophilin unfolding and refolding (Liu, C., Gaspar, J. A., Wong, H. J., and Meiering, E.M, unpublished data) are also best fit using nonlinear denaturant dependence of $\Delta G_u(T,[\text{urea}])$. Similar upward curvature of $\Delta G_u(T,[\text{urea}])$ with decreasing urea concentration has been observed for other proteins (*28*, *54*). This raises the often discussed issue of whether LEM is appropriate for analysis of equilibrium denaturation curves. Interestingly, fitting of data for hisactophilin using BEM gives coefficients that are rather similar to values obtained for barnase (*28*) (from Figure 8, 2.65 vs 2.12 for m_1, and 0.080 versus 0.072 for m_2, for barnase and hisactophilin, respectively). Also, data for SH3 domains have been fit using a value of 0.08295 for m_2 (*42*, *54*). This suggests that the curvature could be a general effect of urea, and curves could be fit using BEM by fixing m_2 as was done for SH3. We have therefore included BEM fitting in Table 1, using the value of $m_2 = 0.072$ obtained from Figure 8 in a modified form of eq 1:

$$Y = \frac{Y_N - \langle Y_N - (Y_U + S_U[\text{urea}])\rangle \exp\left(\frac{-\Delta G_u^{H_2O} + m_1[\text{urea}] - m_2[\text{urea}]^2}{RT}\right)}{1 + \exp\left(\frac{-\Delta G_u^{H_2O} + m_1[\text{urea}] - m_2[\text{urea}]^2}{RT}\right)} \quad (14)$$

In general, values of $\Delta G_u^{H_2O}$ obtained using LEM are systematically lower than values obtained by BEM. The differences are very small under conditions where the protein is unstable at low pH; however, the differences increase with increasing pH to ~2 kcal mol^{-1} at pH ~8.7. Although DBM fitting can also account for nonlinear denaturant dependence of ΔG_u (*21*, *22*), using this method for hisactophilin does not give reliable results because there are problems with convergence of fits, and the fitted values are out of line with values obtained for other proteins (*21*). Thus, BEM appears to be the most appropriate method for analysis of urea denaturation curves of hisactophilin.

In conclusion, we have reported herein extensive measurements of the thermodynamic stability of hisactophilin. The data can be fit to two-state chemical- and temperature-induced unfolding models. Stability is strongly pH-dependent and is correlated with the pH dependence of actin- and membrane-binding by hisactophilin. Ionization of histidine residues is implicated in the pH dependence of stability and function, and in the occurrence of cold unfolding under mild solution conditions. Near physiological pH, the stability of hisactophilin is moderate and comparable to the stability of other β-trefoil proteins. The experiments reported herein provide the groundwork for ongoing studies of the dynamics and folding of hisactophilin, which should provide further insights into the molecular determinants of the β-trefoil fold.

ACKNOWLEDGMENT

We thank Harold Frey for assistance with DSC experiments, and Joe Gaspar and Jessica Rumfeldt for helpful discussions.

REFERENCES

1. Scheel, J., Ziegelbauer, K., Kupke, T., Humbel, B. M., Noegel, A. A., Gerisch, G., and Schleicher, M. (1989) *J. Biol. Chem. 264*, 2832−9.
2. Hanakam, F., Albrecht, R., Eckerskorn, C., Matzner, M., and Gerisch, G. (1996) *EMBO J. 15*, 2935−43.
3. Hanakam, F., Gerisch, G., Lotz, S., Alt, T., and Seelig, A. (1996) *Biochemistry 35*, 11036−44.
4. Hanakam, F., Eckerskorn, C., Lottspeich, F., Muller-Taubenberger, A., Schafer, W., and Gerish, G. (1995) *J. Biol. Chem. 270*, 596−602.
5. Stoeckelhuber, M., Noegel, A. A., Eckerskorn, C., Kohler, J., Rieger, D., and Schleicher, M. (1996) *J. Cell Sci. 109*, 1825−1835.
6. Schleicher, M., Andre, B., Andreoli, C., Eichinger, L., Haugwitz, M., Hofmann, A., Karakesisoglou, J., Stockelhuber, M., and Noegel, A. A. (1995) *FEBS Lett. 369*, 38−42.
7. Hammond, M. S., Houliston, R. S., and Meiering, E. M. (1998) *Biochem. Cell Biol. 76*, 294−301.
8. Habazettl, J., Gondol, D., Wiltscheck, R., Otlewski, J., Schleicher, M., and Holak, T. A. (1992) *Nature 359*, 855−8.
9. Murzin, A. G., Brenner, S. E., Hubbard, T., and Chothia, C. (1995) *J. Mol. Biol. 247*, 536−40.
10. Craig, S., Schmeissner, U., Wingfield, P., and Pain, R. H. (1987) *Biochemistry 26*, 3570−6.
11. Chrunyk, B. A., and Wetzel, R. (1993) *Protein Eng. 6*, 733−8.
12. Varley, P., Gronenborn, A. M., Christensen, H., Wingfield, P. T., Pain, R. H., and Clore, G. M. (1993) *Science 260*, 1110−3.
13. Makhatadze, G. I., Clore, G. M., Gronenborn, A. M., and Privalov, P. L. (1994) *Biochemistry 33*, 9327−32.
14. Heidary, D. K., Gross, L. A., Roy, M., and Jennings, P. A. (1997) *Nat. Struct. Biol. 4*, 725−31.
15. Finke, J. M., Roy, M., Zimm, B. H., and Jennings, P. A. (2000) *Biochemistry 39*, 575−83.
16. Clementi, C., Jennings, P. A., and Onuchic, J. N. (2000) *Proc. Natl. Acad. Sci. U.S.A. 97*, 5871−6.
17. Estape, D., van den Heuvel, J., and Rinas, U. (1998) *Biochem. J. 335*, 343−9.
18. Estape, D., and Rinas, U. (1999) *J. Biol. Chem. 274*, 34083−8.
19. Murzin, A. G., Lesk, A. M., and Chothia, C. (1992) *J. Mol. Biol. 223*, 531−43.
20. Baker, D. (2000) *Nature 405*, 39−42.
21. Pace, C. N. (1986) *Methods Enzymol. 131*, 266−80.
22. Tanford, C. (1970) *Adv. Protein Chem. 24*, 1−95.
23. Gill, S. C., and von Hippel, P. H. (1989) *Anal. Biochem. 182*, 319−26.
24. Winder, A. F., and Gent, W. L. (1971) *Biopolymers 10*, 1243−51.
25. Good, N. E., Winget, G. D., Winter, W., Connolly, T. N., Izawa, S., and Singh, R. M. (1966) *Biochemistry 5*, 467−77.
26. Matouschek, A., Matthews, J. M., Johnson, C. M., and Fersht, A. R. (1994) *Protein Eng. 7*, 1089−95.
27. Privalov, P. L., and Potekhin, S. A. (1986) *Methods Enzymol. 131*, 4−51.
28. Johnson, C. M., and Fersht, A. R. (1995) *Biochemistry 34*, 6795−804.
29. Becktel, W. J., and Schellman, J. A. (1987) *Biopolymers 26*, 1859−77.
30. Venyaminov, S. Y., and Yang, J. T. (1996) In *Circular Dichroism and the Conformational Analysis of Biomolecules* (Fasman, G. D., Ed.) pp 69−109, Plenum Press, New York.
31. Woody, R. W., and Kunker, A. K. (1996) In *Circular Dichroism and the Conformational Analysis of Biomolecules* (Fasman, G. D., Ed.) pp 109−158, Plenum Press, New York.
32. Perczel, A., and Hollosi, M. (1996) In *Circular Dichroism and the Conformational Analysis of Biomolecules* (Fasman, G. D., Ed.) pp 285−380, Plenum Press, New York.
33. Privalov, P. L. (1990) *Crit. Rev. Biochem. Mol. Biol. 25*, 281−305.
34. Privalov, P. L. (1979) *Adv. Protein Chem. 33*, 167−241.

35. Santoro, M. M., and Bolen, D. W. (1992) *Biochemistry 31*, 4901−7.
36. Pace, C. N., and Laurents, D. V. (1989) *Biochemistry 28*, 2520−5.
37. Scholtz, J. M. (1995) *Protein Sci. 4*, 35−43.
38. Makhatadze, G. I., and Privalov, P. L. (1992) *J. Mol. Biol. 226*, 491−505.
39. Pace, C. N., Laurents, D. V., and Thomson, J. A. (1990) *Biochemistry 29*, 2564−72.
40. Pace, C. N., Laurents, D. V., and Erickson, R. E. (1992) *Biochemistry 31*, 2728−34.
41. Taddei, N., Chiti, F., Paoli, P., Fiaschi, T., Bucciantini, M., Stefani, M., Dobson, C. M., and Ramponi, G. (1999) *Biochemistry 38*, 2135−42.
42. Filimonov, V. V., Azuaga, A. I., Viguera, A. R., Serrano, L., and Mateo, P. L. (1999) *Biophys. Chem. 77*, 195−208.
43. Meiering, E. M., Serrano, L., and Fersht, A. R. (1992) *J. Mol. Biol. 225*, 585−9.
44. Jackson, S. E. (1998) *Fold. Des. 3*, R81−91.
45. Chrunyk, B. A., Evans, J., Lillquist, J., Young, P., and Wetzel, R. (1993) *J. Biol. Chem. 268*, 18053−61.
46. Makhatadze, G. I., and Privalov, P. L. (1995) *Adv. Protein Chem. 47*, 307−425.
47. Myers, J. K., Pace, C. N., and Scholtz, J. M. (1995) *Protein Sci. 4*, 2138−48.
48. Privalov, P. L., Griko Yu, V., Venyaminov, S., and Kutyshenko, V. P. (1986) *J. Mol. Biol. 190*, 487−98.
49. Liu, Y., and Sturtevant, J. M. (1996) *Biochemistry 35*, 3059−3062.
50. Chiti, F., van Nuland, N. A., Taddei, N., Magherini, F., Stefani, M., Ramponi, G., and Dobson, C. M. (1998) *Biochemistry 37*, 1447−55.
51. Griko, Y. V., and Privalov, P. L. (1992) *Biochemistry 31*, 8810−5.
52. Agashe, V. R., and Udgaonkar, J. B. (1995) *Biochemistry 34*, 3286−99.
53. Nicholson, E. M., and Scholtz, J. M. (1996) *Biochemistry 35*, 11369−78.
54. Viguera, A. R., Serrano, L., and Wilmanns, M. (1996) *Nat. Struct. Biol. 3*, 874−80.
55. Perrin, D. D., and Dempsey, B. *Buffers for pH and Metal Ion Control*, pp , 285−380, Chapman and Hall Ltd, London.

BI002609I